



NUMERICAL INVESTIGATION OF THE SUCTION AND BLOWING EFFECTS ON THE PERFORMANCE OF S826 AEROFOIL FOR WIND TURBINE APPLICATIONS

Aljunayd Aloukili^{1,3*}, Mohamed Elsakka², Mostafa Ali³, M. Elfaisal Elrefaie³

¹Mechanical Engineering Department, Faculty of Engineering, University of Derna, Derna, Libya.

²Mechanical Power Engineering Department, Faculty of Engineering, Port Said University, Port Said, Egypt.

³Mechanical Power Engineering Department, Faculty of Engineering, Al-Azhar University, Cairo, Egypt.

*Correspondence: aljonaid.mohammed@uod.edu.ly

Citation:

A. Aloukili, M. Elsakka, M. Ali and M.E. Elrefaie, "Numerical investigation of the suction and blowing effects on the performance of s826 aerofoil for wind turbine applications ", Journal of Al-Azhar University Engineering Sector, vol. 19, pp. 117 - 130, 2024.

Received: 02 December 2023

Revised: 04 January 2024

Accepted: 20 January 2024

DOI:10.21608/aej.2024.253920.1510

Copyright © 2024 by the authors. This article is an open-access article distributed under the terms and conditions of Creative Commons Attribution-Share Alike 4.0 International Public License (CC BY-SA 4.0)

ABSTRACT

There is an increasing research focus on improving the efficiency of wind turbines. By employing suction and blowing as methods to manipulate the boundary layer, it is possible to address problems like separation and stall, resulting in enhanced lift production, less drag, and an overall increase in turbine efficiency. This research examines the influence of suction and blowing on the boundary layer of a specific wind turbine aerofoil, to analyze their impact on the overall aerodynamic performance. Computational Fluid Dynamics simulations, utilizing the RANS equations and the SST k- ω turbulence model, are utilized to obtain a more profound understanding of the impact of suction and blowing on the flow field surrounding the aerofoil. The computational fluid dynamics (CFD) results are compared to recently published experimental data to confirm their accuracy and reliability. The aerofoil's performance is evaluated by testing it at the angle of attacks ranging from 0 to 20°. The S826 aerofoil is selected for the current analysis. The inquiry involves analyzing the effects of suction and blowing on lift and drag coefficients. The lift and drag coefficients of the aerofoil are assessed at different blowing and suction flow rates. Although the suction and blowing may increase the lift coefficient of the aerofoil, it has been observed that it can enhance the lift-to-drag ratio in specific situations. The findings demonstrate the impact of suction and blowing processes on the properties of the boundary layer, underscoring the significance of meticulously choosing the rates of suction and blowing mass flow.

KEYWORDS: wind turbine ,boundary layer control, S826 aerofoil, separation and stall, lift to drag ratio.

دراسة عددية لتأثيرات الشفط والنفخ على أداء المقطع الإسيابي S826 لتطبيقات تربينات الرياح

الجنيد العوكلي^{1,3*}، محمد السقا²، مصطفى علي³، محمد الفيصل الرفاعي³

¹قسم الهندسة الميكانيكية، كلية الهندسة، جامعة درنة، درنة، ليبيا

²قسم هندسة القوي الميكانيكية، كلية الهندسة، جامعة بورسعيد، بورسعيد، مصر

³قسم هندسة القوي الميكانيكية، كلية الهندسة، جامعة الأزهر، القاهرة، مصر.

*البريد الإلكتروني للباحث الرئيسي : aljonaid.mohammed@uod.edu.ly

NUMERICAL INVESTIGATION OF THE SUCTION AND BLOWING EFFECTS ON THE PERFORMANCE OF S826 AEROFOIL FOR WIND TURBINE APPLICATIONS

المخلص

هناك اهتمام بحثي متزايد لتحسين أداء توربينات الرياح. يساعد استخدام الشفط والنفخ كآليات تحكم في الطبقة الحدودية على تخفيف مشكلات مثل الانفصال والتوقف، مما يؤدي إلى تحسين توليد الرفع، وتقليل السحب، وزيادة إجمالية في كفاءة التربينات. تتعمق هذه الورقة في تأثير الشفط والنفخ على الطبقة الحدودية للمقطع الإنسيابي المختار لتربينات الرياح، بهدف تحليل آثارها على الأداء الإيروديناميكي العام. تُستخدم عمليات محاكاة ديناميكيات الموائع الحسابية، استنادًا إلى معادلات RANS ونموذج الاضطراب $k-\omega$ SST، للحصول على رؤى أعمق حول تأثيرات الشفط والنفخ على مجال التدفق حول المقطع الإنسيابي. يتم التحقق من صحة النتائج العددية مقابل البيانات التجريبية المنشورة مؤخرًا. يتم تقييم أداء المقطع الإنسيابي بزوايا هجوم تتراوح بين 0 و 20 درجة. في هذه الدراسة، تم اختيار المقطع الإنسيابي S826 للفحص، نظرًا لتطبيقه على نطاق واسع في أشكال تربينات الرياح. يشمل البحث تحليل تأثير كلا من عمليتي الشفط والنفخ على معاملات الرفع والسحب. يتم تقييم معاملات الرفع والسحب للمقطع الإنسيابي عند معدلات تدفق النفخ والشفط المختلفة. في حين أن الشفط والنفخ قد يزيدان من معامل الرفع للمقطع الإنسيابي، فقد وجد أنه يزيد من نسبة الرفع إلى السحب في سيناريوهات معينة. تكشف النتائج عن تأثير آليات الشفط والنفخ على خصائص الطبقة الحدودية، مع التأكيد على أهمية الاختيار الدقيق لمعدلات تدفق الكتلة المتدفقة والشفط.

الكلمات المفتاحية: تربينات الرياح، التحكم في الطبقة الحدودية، المقطع الإنسيابي S826، الانفصال والتوقف، نسبة الرفع للسحب.

1. INTRODUCTION

Lack of fossil fuel resources [1], an increase in greenhouse gas emissions, the IPCC 1.5°C increase scenario, and other institutions interested in environmental affairs [2], [3], and the excessive need for additional energy sources [4], encouraged the research filed to offer additional efforts in the renewable energy sources and ventilation sectors enhancement.

Earth is endowed with a rich variety of renewable energy sources. Among these, solar energy, wind energy, and geothermal energy stand out as exemplary illustrations of diverse and sustainable energy options. [5]. Putting wind energy under the scope of research, a variation in wind velocities over the world has been noticed as shown in the following wind atlas [6]. Locations with high wind velocities were already used to produce energy, and with time the world will need to use moderate and low wind speed velocities regions [7].

Wind turbines are devices frequently employed to capture energy from the atmospheric wind. These turbines fall into two primary categories: horizontal-axis wind turbines and vertical-axis wind turbines. The windmill turbines and the three-blade turbines could be considered as horizontal axis turbines, and the Savonius turbines and the Darrius turbines could be considered as vertical axis wind turbines [8].

Each wind turbine has a range of tip speed ratio (TSR) where that turbine gives the highest performance[9]. When a fluid stream flows around a chambered body, the flow experiences two types of parameter changes, pressure, and velocity, which are well known as favorable pressure gradient and unfavorable pressure gradient. The unfavourable pressure gradient region witnesses a worldwide known phenomenon, which is the separation of flows. The separation phenomenon causes a wake, which is an area of flow swirls characterized by high flow velocity and low pressure [10].

Such a phenomenon causes a high drag force over the submerged body. Aerofoils are one of these submerged bodies. The drag forces are not needed for most applications where aerofoils are utilized such as wind turbines and aircraft, where lift force is more required and high esteem of

NUMERICAL INVESTIGATION OF THE SUCTION AND BLOWING EFFECTS ON THE PERFORMANCE OF S826 AEROFOIL FOR WIND TURBINE APPLICATIONS

drag force is not a delightful occasion [11]. Lift and drag forces are concurrently generated on the surface of an aerofoil. The lift force, widely acknowledged as the primary useful force, experiences a detrimental impact from the separation phenomenon. This occurrence leads to an increase in drag force, thereby diminishing the efficiency of the aerofoil [12].

As this work is more directed toward wind turbines, more information on the effect of separation on turbine performance will be presented. It is found through many previous works that increasing the attack angle of an aerofoil increases the power coefficient produced by a turbine until a specific angle value which is ideally known as stall angle. The stall angle limits the increase of power extracted by the turbine as the flow stream at this point is separated from the aerofoil body so no moment exchange will occur. The stall is known to happen when a sudden reduction in lift force accompanied by a sudden increase in drag force is noticed [13].

Multiple configurations were created to delay the separation or even better overcome this phenomenon. One of these efforts was jet blowing and suction, the main idea behind jet blowing and suction is to add external moment to the flow stream over the aerofoil to its residual moment, which no longer can adhere to the aerofoil wall furthermore exchange moment, This additional moment helps flow stream to adhere to the aerofoil wall much longer and increase the stall angle hence increasing the capability of the aerofoil to produce higher lift force value and as result in higher power coefficients [14], [15]. An experimental study was performed on the NACA0012 aerofoiled blade and studied the effects of perpendicular blowing and suction jets holes geometry at $Re = 1 \times 10^5$ and turbulence intensity less than 0.5%. The holes were distributed at 0.2 and 0.3 of the cord length for blowing, with an inner diameter of 1 mm and a row width of 0.93 of the span length. By varying the momentum coefficient C_m , which characterizes the jet intensity [14].

The experimental data for blowing led to the following results, while all C_m values contribute to drag reduction across the blade, it is noteworthy that the smallest C_m values possess the distinct capability to significantly enhance lift values. Locating the blowing jet holes at 0.2 of the cord length and with $C_m = 0.104$ enhanced the lift coefficient C_L by 18.4% and a 4-degree stall angle delay was achieved. However, 0.3 of the chord length did not achieve C_L enhancement over the base blade, and a 2-degree stall delay was achieved. The blowing-suction control showed a weaker control due to the suction slot's ability to reattach the flow immediately, which created turbulence bubbles, thus providing additional drag over the blade and minimal enhancement in the C_L value [14]. A CFD investigation was performed over the impact of blowing jet velocity over different aerofoils, NACA0012 and LA203A, at $Re = 5 \times 10^5$ and $Ma = 0.2$ at a constant location corresponding to 0.6 times the chord length and with varying angles of attack, the blowing ratio (A), which is defined as the ratio of the jet velocity to the free stream velocity, ranging from 0 to 0.4 was investigated. The NACA0012 showed noticeable enhancement in the C_L values, hence fine boundary layer control, and stall angle delay of 4 degrees [16].

The maximum C_L value was enhanced by 3.97% at $A=0.2$ for the NACA aerofoil. However, for the LA203A aerofoil, the max C_L value was enhanced by 0.72% at $A=0.2$ with a stall angle delay of 2 degrees. Elevated blowing ratios caused the free stream to travel at a distance from the boundary layer, impeding the vortices generated by the jet stream from reaching the free stream and exchanging momentum. Moreover, a continued increase in the blowing ratio heightened the jet

NUMERICAL INVESTIGATION OF THE SUCTION AND BLOWING EFFECTS ON THE PERFORMANCE OF S826 AEROFOIL FOR WIND TURBINE APPLICATIONS

stream moment to a degree where the mainstream could no longer synchronize with the jet stream, resulting in a reduction of the C_L value [16].

A CFD investigation was conducted by [15] to enhance the performance of a NACA0012 aerofoil. The enhancement was designed to be achieved by employing either parallel and tangential blowing near the trailing edge or parallel and tangential suction near the leading edge. The parameters under scope were the jet location, jet width, and jet stream velocity. It was agreed that a parallel injection stream with a blowing ratio higher than 0.2 causes a reduction in the C_L and enhances the C_D for the aerofoil. Moreover, for a parallel injection jet, a narrow width, roughly around 1.5% of the chord length, boosts the enhancement of the airfoil [15-16].

It was found that a tangential-blowing jet is more effective for flow injection near the trailing edge when utilizing a high blowing ratio and a substantial jet width of approximately 0.5 and 4% of the chord length, respectively. Although the tangential blowing jet achieved an enhancement in C_L of 7% and a reduction in C_D by 7% at angle of attack (AoA) = 14, the perpendicular blow jet, under the mentioned conditions of the case study, caused a reduction in C_L and C_D by 23% and 16% at AoA = 14, respectively. The effect of the suction jet with $A = 0.5$, $H = 2.5\%$, the location of suction jet with respect to the chord length $(X/C)_s = 0.1$ from the leading edge, and AoA = 18 degrees enhanced C_L by 75% and decreased $C_D = 56\%$ [15]. A Direct Numerical Simulation (DNS) was carried out to optimize the pulsed jet configuration aimed at controlling flow separation over a NACA0012 airfoil. The optimization process was performed under specific conditions, $Re = 105$, $Ma = 0.2$, $A = 0.4$, AoA = 2 degrees, two dimensionless frequencies (F^+), $F^+ = FC/U_\infty$, of 2 and 1.5, and two jet geometries, perpendicular jet with the suction surface and tilted jet of 30 degrees with the suction surface, as two different case studies [17].

The investigation showed that the optimized condition for injection is at a position right before the separation occurs over the blade suction surface which is for the NACA0012 at $X/C = 0.19$, tilting the jet port by an angle of 30 degrees with the surface of the aerofoil, using the low value of $F^+ = 1.5$, and using too small and very sharp port for the jet. These conditions caused a reduction in the C_D by 81.43%, kept the C_L value almost constant, and reduced the separation area and the maximum reverse flow velocity from 30% U_∞ at the base case to 2% U_∞ at the optimized case, and the required mass flow rate is also reduced, which allow the pulsed jet to deal with the early formed separation region [17]. An experimental test was conducted on the NACA0025 aerofoil to investigate the influence of varying the dimensions of blowing and suction on the aerodynamic performance of the airfoil. The experiment came up with results that the thin-blowing jet port is lower in performance than the large-blowing jet port. However, the fact that a large-blowing port requires 4 times the power required for the thin port to achieve minimal enhancement in C_L is not avoidable, this made the thin-blowing port a better arrangement [18].

Results also went along with the previously mentioned CFD and experimental investigations that a $C_m = 0.2$ is preferred for operation enhancement. The experiment was performed for an aerofoil where the suction port was designed with divergent path and the blowing port was designed with divergent path, which plays a role in the enhancement of the suction and blowing paths aerodynamics. Ports also were tilted at an angle of 40 degrees and the port's locations were $(X/C)_B = 0.074$, $(X/C)_S = 0.83$. The provided design for the experiment enhanced C_L by 220% and reduced C_D by 127% at $C_m = 0.2$ [18].

NUMERICAL INVESTIGATION OF THE SUCTION AND BLOWING EFFECTS ON THE PERFORMANCE OF S826 AEROFOIL FOR WIND TURBINE APPLICATIONS

A numerical simulation was performed to analyze the impacts of concurrent blowing and suction on the NREL S809 airfoil. The blowing jet was positioned at 6% of the chord length from the leading edge, with a height of 0.65% of the chord length. Additionally, the suction port was situated at 80% of the chord length from the leading edge, with a height of 1.38% of the chord length. The arrangement investigated at conditions of $Ma = 0.076$, $Re = 10^6$, and $C_m = 0.12$ enhanced the C_L by 51.14%, reduced the C_D by 78.01% and power performance efficiency was 62.18% [19]. An experimental test on the NACA6415 for the open CFJ (OCFJ) and discrete CFJ (DCFJ) was performed at $Re = 1.95 \times 10^5$ and $U_{00} = 10$ m/s, the data for blowing and suction slots are as follows 7.5%C with 0.65%C height and 88.5%C with 1.42%C height, respectively. At a mass flow rate of 0.060 Kg/s (the jet momentum coefficient for the open slot [C_m^*] = 0.25) at DCFJ with Obstruction Factor (OF) 3/4 enhanced C_L by 250%. It was noticed from the experimental results that DCFJ enhances C_L by 50%, reduces C_D by 300%, and 30% increase in AoA compared to the OCFJ performance. However, OCFJ is 10 times less power consumption compared to the DCFJ [20]. Numerical methods were employed to investigate the aerodynamic performance of a selection of various profiles utilized as blades. Given the low Reynolds number, the present study specifically centers on the performance of vertical axis wind turbines. The investigation delved into stall and separation effects, aiming to establish guidelines for utilizing a specific aerofoil within a defined range of speeds to achieve optimal power coefficient [21].

2. Numerical simulation

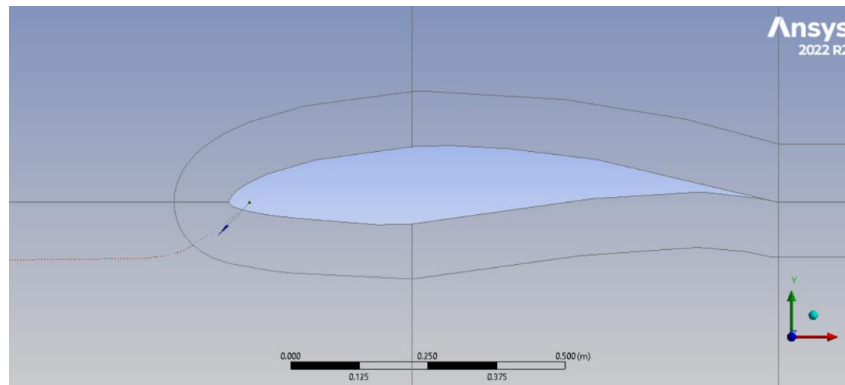
2.1. Turbulent model and governing equations

The ANSYS simulation program was employed to conduct a Computational Fluid Dynamics (CFD) simulation on the chosen wind turbine airfoils featuring blowing and suction jets. The incorporation of these components aimed to refine the aerodynamics of the airflow over the wind turbine's airfoils. The simulation utilized the Reynolds-Averaged Navier-Stokes (RANS) approach within the FLUENT code, accounting for mass, energy, momentum, and state governing equations under unsteady, incompressible assumptions. Moreover, the simulation incorporated the SST K- ω turbulence model with a turbulence intensity of 5%, relying on dissipation rate and turbulent kinetic energy for accurate representation.

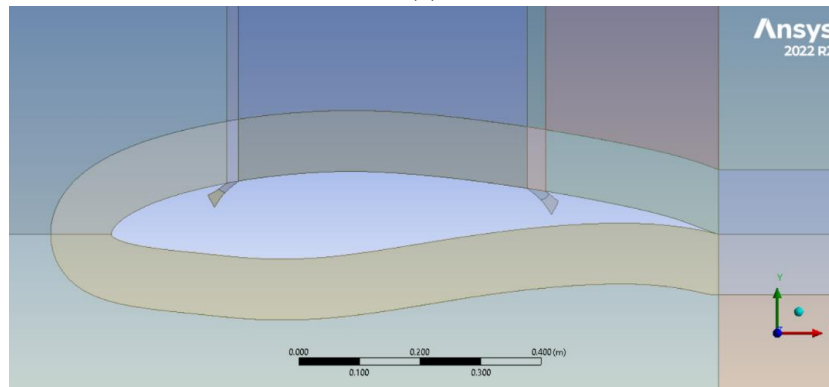
2.2. Geometry and computational domain

NREL S826 aerofoil is selected to be used for this case study. The augmenting blowing and suction jets are generated at positions 0.2 and 0.7 of the chord length, respectively, measured from the leading edge. The blowing slot depth is 2% of the aerofoil cord, the suction slot is designed to have a depth of 3% of the cord, and the blowing slot angle is set to be at 35° with respect to X axis, while the suction slot angle is set to be at 133° with respect to X axis. **Figure 1** shows both the base NREL S826 aerofoil and the simulated configuration.

NUMERICAL INVESTIGATION OF THE SUCTION AND BLOWING EFFECTS ON THE PERFORMANCE OF S826 AEROFOIL FOR WIND TURBINE APPLICATIONS



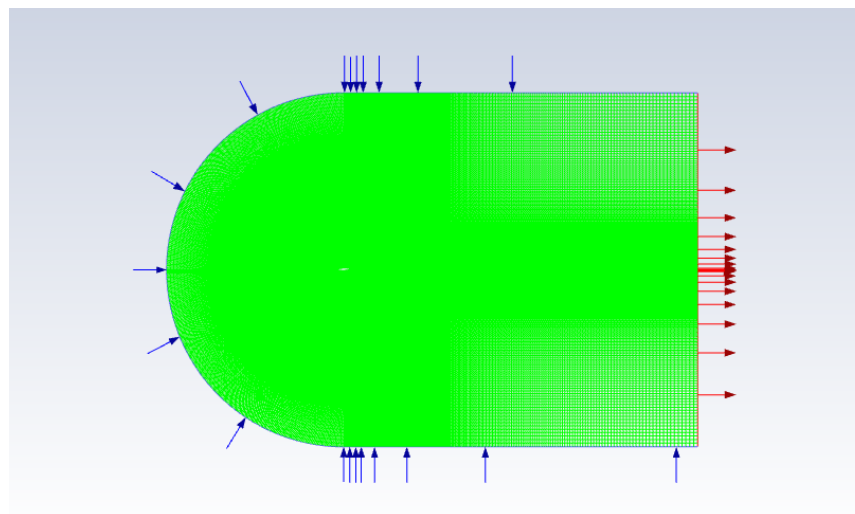
(a)



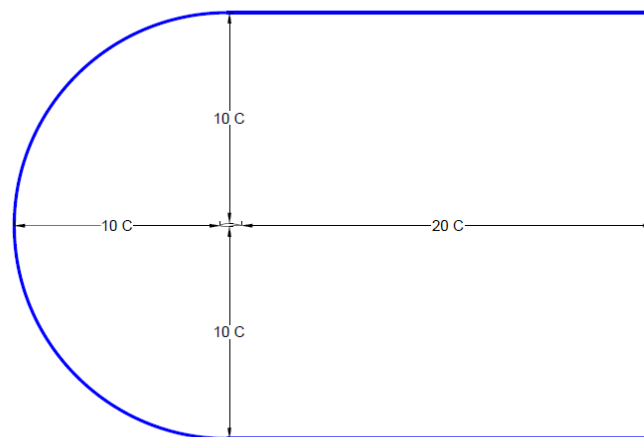
(b)

Figure 1: The geometrical configuration of a) Base NREL S826aerofoil and b) NREL S826 with augmented blowing and suction.

NUMERICAL INVESTIGATION OF THE SUCTION AND BLOWING EFFECTS ON THE PERFORMANCE OF S826 AEROFOIL FOR WIND TURBINE APPLICATIONS



(a)



(b)

Figure 2: The computational domain for the simulation of NREL S826 aerofoil with augmented blowing and suction.

The input velocity and outlet pressure domains are set at a distance of 10 chord lengths from the leading edge and 20 chord lengths from the trailing edge. The 10 chord lengths of the aerofoil remain consistent within the symmetric domain, excluding the suction and pressure sides. Such dimensions are chosen to ensure that the computational domain boundary will not affect the flow field during the numerical calculation. **Figure 2** illustrates the computational domain boundary around the NREL S826 aerofoil.

The common considerations for meshing are taken into account in order to ensure high-quality results, the mesh is generated by ANSYS Meshing CFD. The quantity of mesh cells is denser near the wall of the aerofoil to ensure better simulation for the boundary-varied characteristics. **Figure 3** shows the mesh of the NREL S826 aerofoil with blowing and suction, and base configurations. Various mesh numbers are tested to configure the most suitable mesh number where variations are as small as possible and the mesh number of 340700 is found to be optimal for

NUMERICAL INVESTIGATION OF THE SUCTION AND BLOWING EFFECTS ON THE PERFORMANCE OF S826 AEROFOIL FOR WIND TURBINE APPLICATIONS

the simulation as increasing the cell number makes negligible difference, and the simulation is performed at Reynolds number (Re) equal to 6×10^5 . Blowing and suction variations of momentum coefficient (C_m) are put under study where

$$C_m = \frac{\dot{m}_j V_j}{0.5 \rho U_\infty^2 S}$$

Where:

C_m : momentum coefficient

\dot{m}_j : jet mass flow rate

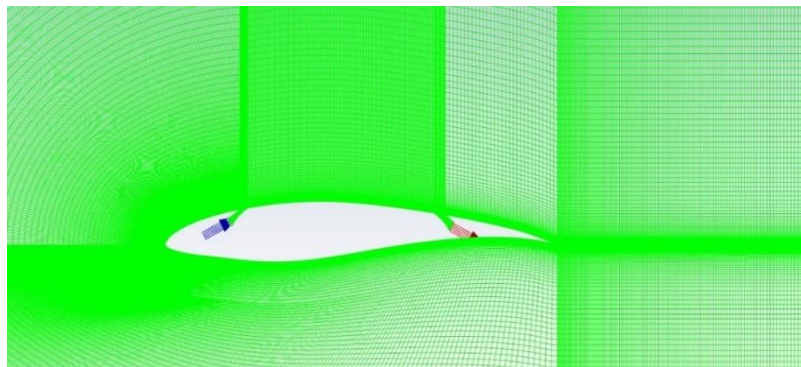
V_j : jet velocity

ρ : air density

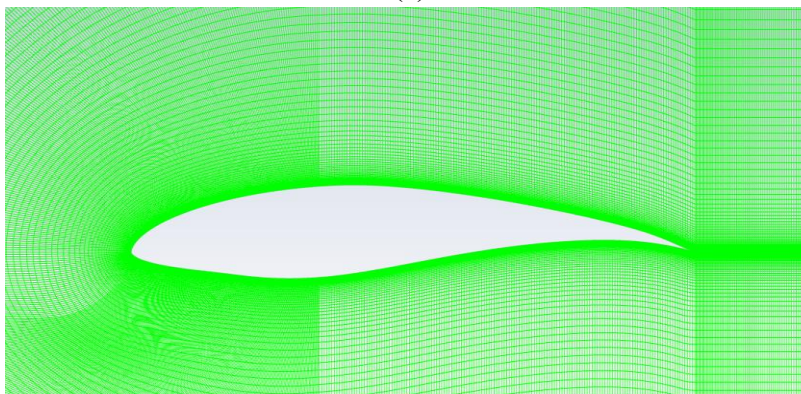
U_∞^2 : ambient air velocity

S : the aerofoil area

while the blowing and suction are characterized to be the same. The C_m are varied in the range of 0.08, 0.16, 0.2, 0.4 and 0.5 which correspond to the flow rate values of 0.31, 0.43, 0.49, 0.68 and 0.76 Kg/s, respectively. A mass flow inlet boundary condition is applied at the entrance of the blowing nozzle, while the mass flow rate is employed to quantify the mass exiting from the suction nozzle exit.



(a)



(b)

Figure 3: The mesh of a) the NREL S826 aerofoil with blowing and suction simultaneously configuration and b) the base NREL S826 aerofoil.

NUMERICAL INVESTIGATION OF THE SUCTION AND BLOWING EFFECTS ON THE PERFORMANCE OF S826 AEROFOIL FOR WIND TURBINE APPLICATIONS

3. Results and discussion

The effect of applying similar momentum coefficients (C_m) for both Suction and blowing, where both are activated simultaneously, on the generated lift and drag over the NREL S826 aerofoil and the stall angle delay are discussed. The C_m values are changing through the given domain of 0.08, 0.16, 0.2, 0.4 and 0.5.

3.1. Model validation:

The base NREL S826 aerofoil model simulation results are validated with the experiment data provided by Barti et al. [22] and they both almost matched. The unmatched results may be due to computational errors. **Figure 4** shows the validation curve where a good match between the given data and the present simulated NREL S826 aerofoil appears around the stall angle of 13° . These results give a kind of credibility to the results presented later.

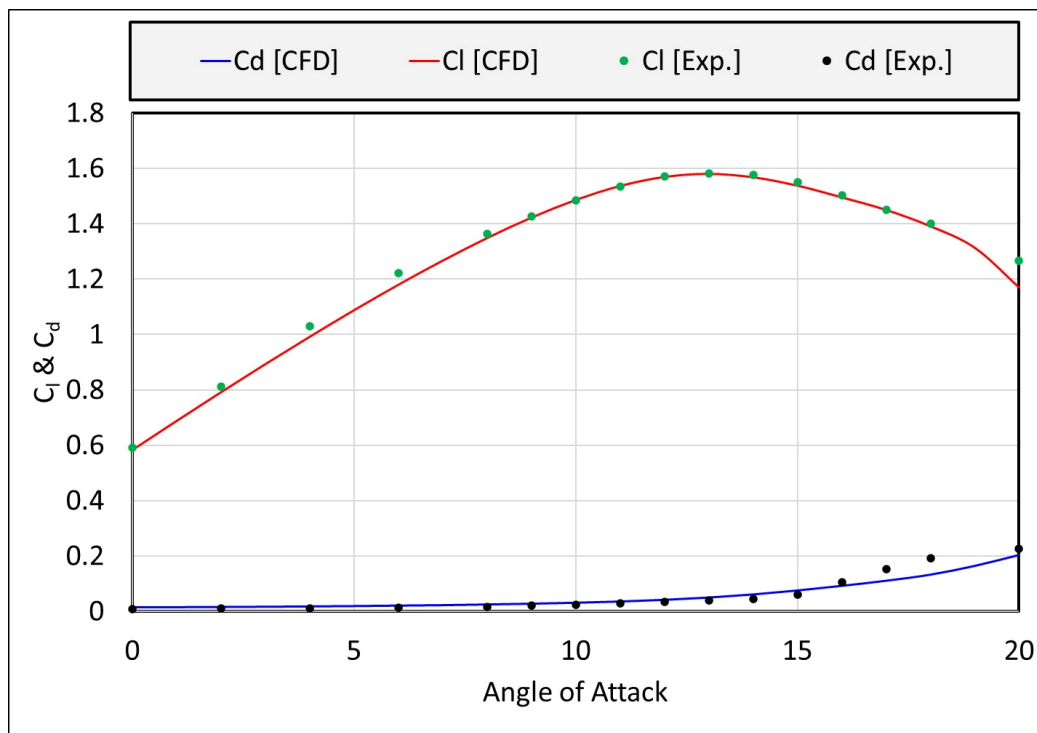


Figure 4: The Validation results between the current study and the experimental data provided by Barti et al. [22], for the same aerofoil at momentum coefficient $C_m = 0$.

3.2. The effect of blowing and suction over the generated lift and drag:

Varying the momentum coefficient (C_m) values for suction and blowing increases the overall performance of the NREL S826 aerofoil from the perspective of generated lift. However, it has almost negligible consequences. **Figure 5** illustrates the effect of applying suction and blowing simultaneously with similar momentum coefficients for both processes. For $C_m = 0.08$ an increase of 49.68% in the generated lift coefficient is obtained at an angle of attack of 13° .

Furthermore, increasing the momentum coefficient leads to a continuous increase in the generated lift over the aerofoil. Where, at the angle of attack of 13° , an increase equal to 63.53%, 78%, 109.44%, and 127.1% in lift coefficient (C_L) for momentum coefficients of 0.16, 0.2, 0.4, and

NUMERICAL INVESTIGATION OF THE SUCTION AND BLOWING EFFECTS ON THE PERFORMANCE OF S826 AEROFOIL FOR WIND TURBINE APPLICATIONS

0.5, respectively. Despite the continuous increase in generated lift over the aerofoil using blowing and suction, financials limit the possibility of the increase in momentum coefficients for blowing and suction techniques.

Stall angle delay is considered the main required consequence of applying blowing and suction to an aerofoil. **Figure 5** also sheds light on postponing the angle of attack at which stall occurs for the same blowing and suction momentum coefficients. For $C_m = 0.08$, a stall delay by a single degree appears whereas for the base condition, the stall appears at an angle of attack equal to 13° . However, the condition with $C_m = 0.08$ applied to the NREL S826 aerofoil, stall occurs at an angle of attack of 14° .

Furthermore, applying a $C_m = 0.16$ and $C_m = 0.2$ to the base NREL S826 aerofoil increases the generated lift. However, the stall angle is not affected, standing at 13° . Enhancements are highly notable for applying $C_m = 0.4$ and $C_m = 0.5$. At $C_m = 0.4$, the stall is delayed by five degrees higher than the base condition making the stall appear at an attack angle of 18° . **Figure 5** shows also a result which is opposite to the expected results for applying $C_m = 0.5$, where the stall angle delaying effect is less than at the $C_m = 0.4$ case. The stall at $C_m = 0.5$ occurs at an attack angle of 17° making a delay by four degrees over the base case.

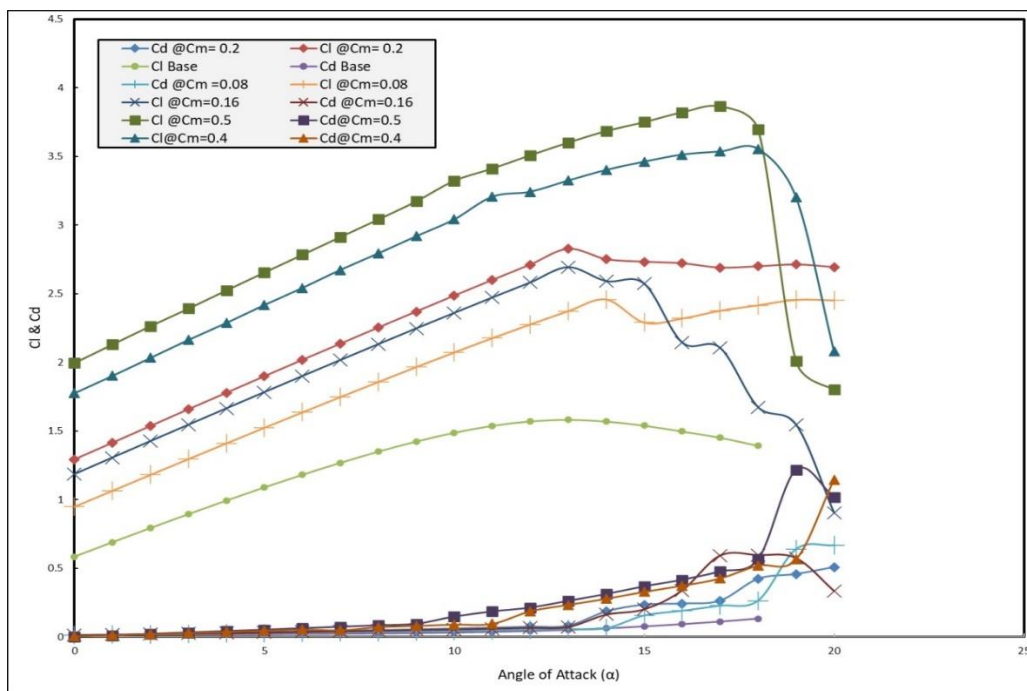
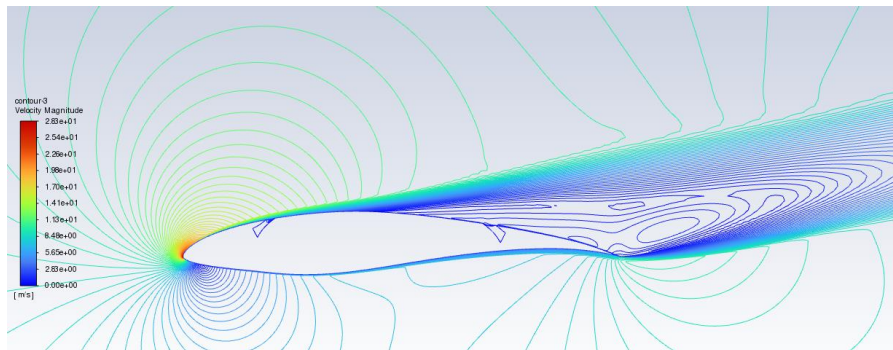


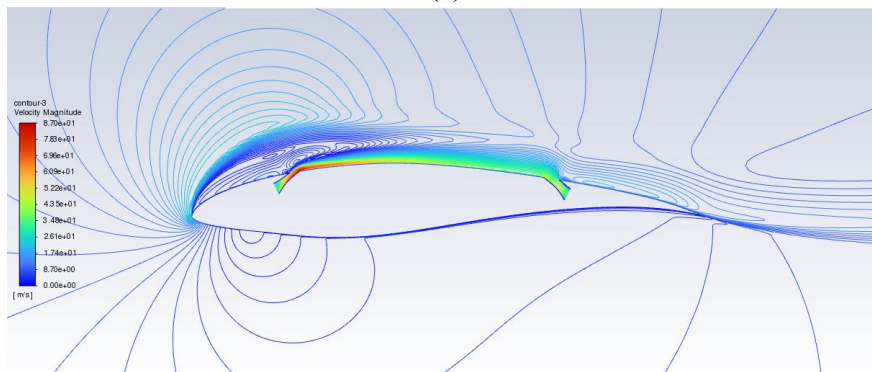
Figure 5: Simulation results for lift and drag coefficients with the variation of momentum coefficient from 0.08 to 0.5.

Figure 6 and 7 show the velocity contour lines that represent a visual illustration of the velocity distribution in the flow field around the aerofoil. These contours illustrate the effect of the simultaneous suction and blowing separation bubble configuration, which can explain the reason behind such enhancements. As shown in **Figure 6**, by applying $C_m = 0.5$, the turbulent bubble formed at the trailing edge is almost eliminated at the angle of attack (AOA) equal to about 17° . **Figure 7** also presents the elimination of turbulent bubbles at the trailing edge when applying $C_m = 0.2$ at $AOA = 13^\circ$, the effect of blowing and suction is obvious.

NUMERICAL INVESTIGATION OF THE SUCTION AND BLOWING EFFECTS ON THE PERFORMANCE OF S826 AEROFOIL FOR WIND TURBINE APPLICATIONS

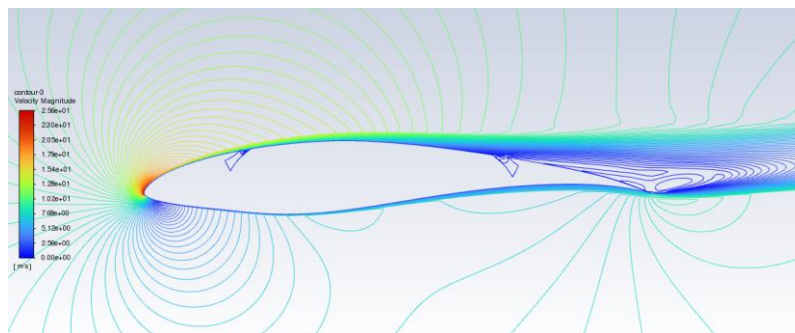


(a)

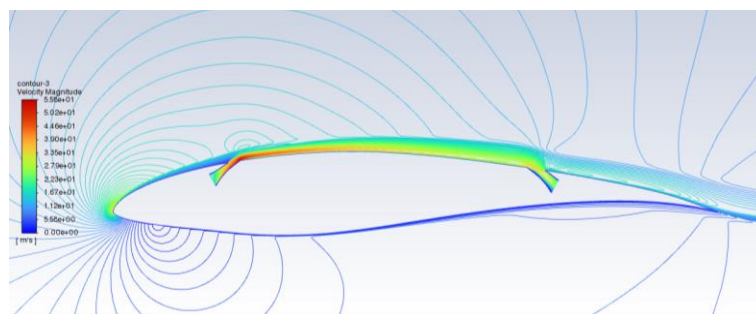


(b)

Figure 6: The contour lines at AOA = 17 for a) Based NREL S826 aerofoil and b) aerofoil NREL S826 with suction and blowing at $C_m = 0.5$.



(a)



(b)

Figure 7: The contour lines at AOA = 13 for a) Based NREL S826 aerofoil and b) aerofoil NREL S826 with suction and blowing at $C_m = 0.2$.

NUMERICAL INVESTIGATION OF THE SUCTION AND BLOWING EFFECTS ON THE PERFORMANCE OF S826 AEROFOIL FOR WIND TURBINE APPLICATIONS

Conclusions

Various previous works illustrated the effect of applying secondary suction and blowing at various flow rates. However, most work efforts were directed to study the NACA aerofoils, applying the blowing and suction at different values of mass flow rate for each. This study focused on configuring the effect of applying simultaneous suction and blowing with the same mass flow rate, expressing its value using the momentum coefficient (C_m), on the NREL S826 aerofoil using CFD simulation techniques.

The NREL S826 aerofoil geometry is designed and validated with the provided experimental data, and the validation came out with a good match between values with small error values. These errors are mainly due to computational errors. Applying both blowing and suction simultaneously over the NREL S826 aerofoil with the same C_m for each at a range of C_m from 0.08 to 0.5 gives the following results.

- Increasing the value of momentum coefficients is accompanied by an increase in the generated lift coefficient. with a negligible increase in drag coefficient.
- High delay of stall is generally detected when increasing values of momentum coefficient except for two cases at $C_m = 0.16$ and 0.2 the stall occurs at the same AoA of the basic profile. Check Fig5.
- The highest value of the lift coefficient in this study is obtained at $C_m = 0.5$, which enhanced the lift coefficient value by 127.1%, while the highest stall delay occurs at the attack angle of 18° at $C_m = 0.4$.
- Although $C_m = 0.2$ or 0.25 have been reported as the optimal value based on NACA aerofoils, the present results reveal that the optimal value is much higher for S826 aerofoil. Hence, farther investigations are required to elaborate the effect of different aerofoil profiles on the associated optimal C_m value.

Nomenclature

AOA: Angle of attack

C: Chord length

C_D : Drag coefficient

CFD: Computational fluid dynamics

C_L : Lift coefficient

C_m : Momentum coefficient

F: Frequency

F^+ : Dimensionless frequency

Ma: Mach number

OF: Obstruction factor

Re: Reynolds number

$X/C)_B$: The location of blowing port with respect to the chord length

$X/C)_S$: The location of suction port with respect to the chord length

NUMERICAL INVESTIGATION OF THE SUCTION AND BLOWING EFFECTS ON THE PERFORMANCE OF S826 AEROFOIL FOR WIND TURBINE APPLICATIONS

References

- [1] Van Asselt, H., Piggot, G., Around, E., Bradley, S., Bushan, C., Gençsü, I., ... & Weikmans, R. (2021). The Production Gap: Governments' planned fossil fuel production remains dangerously out of sync with Paris Agreement limits (2021 Report).
- [2] Masson-Delmotte, V., Zhai, P., Pörtner, H. O., Roberts, D., Skea, J., & Shukla, P. R. (2022). Global Warming of 1.5 C: IPCC special report on impacts of global warming of 1.5 C above pre-industrial levels in context of strengthening response to climate change, sustainable development, and efforts to eradicate poverty. Cambridge University Press.
- [3] Renewable Energy Agency, I. (2023). World Energy Transitions Outlook 2023: 1.5°C Pathway. www.irena.org
- [4] Renewable Energy In Energy Demand. (n.d.). Retrieved October 23, 2023, from https://www.ren21.net/gsr-2023/modules/energy_demand
- [5] Abdelilah, Y., Bahar, H., Criswell, T., Bojek, P., Briens, F., & Feuvre, P. L. (2020). Renewables 2020: Analysis and Forecast to 2025. IEA: Paris, France.
- [6] Elsakka, M. M., Ingham, D. B., Ma, L., Pourkashanian, M., Moustafa, G. H., & Elhenawy, Y. (2022). Response surface optimisation of vertical axis wind turbine at low wind speeds. *Energy Reports*, 8, 10868-10880.
- [7] Wind, I. (2017). IEA wind technology collaboration programme.
- [8] Manwell, J. F., McGowan, J. G., & Rogers, A. L. (2010). *Wind energy explained: theory, design and application*. John Wiley & Sons.
- [9] White, F. M., & Xue, H. (n.d.). *Fluid Mechanics NINTH EDITION*.
- [10] Gerhart, P. M., Gerhart, A. L., & Hochstein, J. I. (n.d.). *Fundamentals of Fluid Mechanics Eighth Edition*. www.Ebook777.com
- [11] Goffert, B., Silva, R. S., Francisco, C. P. F., & Reis, M. L. C. C. (2023). Numerical Study of Flow Control on Simplified High-Lift Configurations. *Journal of Applied Fluid Mechanics*, 16(4), 634-654.
- [12] Mifsud, M., Zimmermann, R., & Görtz, S. (2015). Speeding-up the computation of high-lift aerodynamics using a residual-based reduced-order model. *CEAS Aeronautical Journal*, 6, 3-16.
- [13] Elsakka, M. M., Ingham, D. B., Ma, L., & Pourkashanian, M. (2019). CFD analysis of the angle of attack for a vertical axis wind turbine blade. *Energy Conversion and Management*, 182, 154-165.
- [14] Wang, L., Alam, M. M., Rehman, S., & Zhou, Y. (2022). Effects of blowing and suction jets on the aerodynamic performance of wind turbine airfoil. *Renewable Energy*, 196, 52-64.
- [15] Yousefi, K., Saleh, R., & Zahedi, P. (2014). Numerical study of blowing and suction slot geometry optimization on NACA 0012 airfoil. *Journal of Mechanical Science and Technology*, 28, 1297-1310.
- [16] James, S. E., Suryan, A., Sebastian, J. J., Mohan, A., & Kim, H. D. (2018). Comparative study of boundary layer control around an ordinary airfoil and a high lift airfoil with secondary blowing. *Computers & Fluids*, 164, 50-63.
- [17] Deng, S., Jiang, L., & Liu, C. (2007). DNS for flow separation control around an airfoil by pulsed jets. *Computers & fluids*, 36(6), 1040-1060.
- [18] Zha, G. C., Carroll, B. F., Paxton, C. D., Conley, C. A., & Wells, A. (2007). High-performance airfoil using coflow jet flow control. *AIAA journal*, 45(8), 2087-2090.

NUMERICAL INVESTIGATION OF THE SUCTION AND BLOWING EFFECTS ON THE PERFORMANCE OF S826 AEROFOIL FOR WIND TURBINE APPLICATIONS

- [19] Xu, H. Y., Qiao, C. L., & Ye, Z. Y. (2016). Dynamic stall control on the wind turbine airfoil via a co-flow jet. *Energies*, 9(6), 429.
- [20] Dano, B., Zha, G., & Castillo, M. (2011, January). Experimental study of co-flow jet airfoil performance enhancement using discreet jets. In 49th AIAA aerospace sciences meeting including the new horizons forum and aerospace exposition (p. 941).
- [21] Abul-Ela, S. M., Sayed, I. A., Elrefaie, E. M., “Performance Comparative Study of Low Reynolds Number Airfoils Utilized in Vertical-Axis Wind Turbines,” Accepted research paper for presentation in Al-Azhar 16th International Conference (AEIC 2024).
- [22] Bartl, J., Sagmo, K. F., Bracchi, T., & Sætran, L. (2019). Performance of the NREL S826 airfoil at low to moderate Reynolds numbers—A reference experiment for CFD models. *European Journal of Mechanics-B/Fluids*, 75, 180-192.